The Effects of Electrode Configuration on Omnipolar Electrograms: An In-Silico Approach

MK Jothi Letchumy[1], Joseph Brook[1], Konstantinos Ntagiantas[1], Dimitrios Panagopoulos[1], Nicholas S Peters[1], Danya Agha-Jaffar[1], Norman Qureshi[1], Rasheda A Chowdhury[1,#], Chris D Cantwell[1,#]

[1] Imperial College London, London, United Kingdom

Abstract

Atrial Fibrillation (AF) is the most common cardiac arrhythmia, involving pathological triggers and substrate in the atria. In the clinical catheter laboratory, contact electrograms are an essential tool to characterise AF. Omnipolar electrograms (OE), derived from three or more neighbouring electrodes, are thought to be superior compared to traditional unipolar and bipolar electrograms by eliminating far-field effects and correcting for wavefront incidence angle. However, OEs are yet to be fully characterised and may be influenced by electrode configurations.

We sought to understand the changes in OE morphology under different electrode configurations using 2D simulations of healthy tissue and scarred tissue. Virtual unipolar electrograms (UE) were generated from single electrodes which were used to predict the local electric field and subsequently calculate OEs in cliques of 3, 4, and 6 electrodes. A set of five feature points were identified on each OE to measure changes in OE morphology under different clique configurations.

All time intervals between feature points, except between the first peak and the minimum point, increased with inter-electrode distance. The voltage at the two signal peaks and the minimum point increased, while and amplitude decreased, with increased electrode spacing. The number of electrodes in a clique also influenced OEs morphology. Amplitude and duration between peak 1 and the minimum point did not increase, whilst the other intervals between the feature points and the voltage at the feature points did increase. Additionally, the morphology of the OE signals changed in the presence of fibrosis. OE signals obtained from scarred tissue are more fractionated compared with healthy tissue. The most appropriate inter-electrode distances are between 2mm and 3mm using either three or four electrodes.

1. Introduction

Atrial Fibrillation (AF) is the most prevalent chronic cardiac arrhythmia and it affects more than 1.4 million people in the UK [1,2]. It results in poor atrial function, erratic ventricular activation and reduced function efficiency of the heart. The probability of having AF increases with age and approximately 7 in every 100 people over 65 years are diagnosed with AF [3]. With an increasing global elderly population, this disease is leading to an exponential growth in the expense of treating atrial arrhythmia [3].

Fibrosis has been shown to increase susceptibility to AF and may serve as a critical substrate in the formation and stability of the arrhythmia. Additionally, atrial fibrosis is difficult to reverse and has therefore been considered as a major contributor in the progression from paroxysmal to persistent or permanent AF [4]. The correlation of the degree of atrial fibrosis with the persistence of AF in patients has been demonstrated. Mechanistically, fibrosis causes a decrease in the propagation velocity and leads to increased heterogeneity of electrical conduction [5, 6]. Collagen fibres represent electrical barriers, which can cause asynchronous propagation of electrical activation [7, 8].

The contact electrogram is the primary tool used by the electrophysiologist to diagnose AF. It represents the cumulative electrical activity measured from an electrode in direct contact with the myocardium. It is thought that catheter ablation can be enhanced through utilising recorded EGMs to infer the characteristics of the local myocardium. However, in clinical practice, EGM guided catheter ablation has not shown any improvement to date in preventing AF recurrence over conventional pulmonary vein insolation (PVI) [9]. Currently, EGM guided catheter ablation procedures use electrodes to record unipolar electrograms (UE) and/or bipolar electrograms (BE). UEs are obtained from a single electrode in contact with the myocardium, relative to distant electrode. BEs are obtained through the subtraction of two adjacent UEs [10]. BEs eliminate far-field electrical activation, but are more challenging to interpret as their signal depends on the orientation of the inter-electrode axis to the incident electrical

wavefront [11, 12]. A recently developed technique combines multiple unipolar electrograms to compute an *omnipolar electrogram* (OE), which overcomes these limitations. OEs effectively provide the optimal BEs from a clique of three or more electrodes by correcting for both the far-field effect and the wavefront propagation direction [13].

Many aspects of the signal acquisition influence the morphology of the contact electrograms [14]. This *in silico* study focuses on characterising the influence on OE morphology of inter-electrode distance and the number of electrodes in the clique.

2. Methodology

A structured finite element mesh was used to solve the monodomain equation on a 100 x 100 mm square of human atrial myocardium. The 2D rectangular domains in Figure 1 the healthy and non-healthy representations of the tissue. The colour bars indicate the conductivity throughout the domain, applied in the diffusivity tensor of the monodomain equation. The physiological conductivity used ranges from 0.03 mS/mm (scar) to 0.13 mS/mm (healthy).

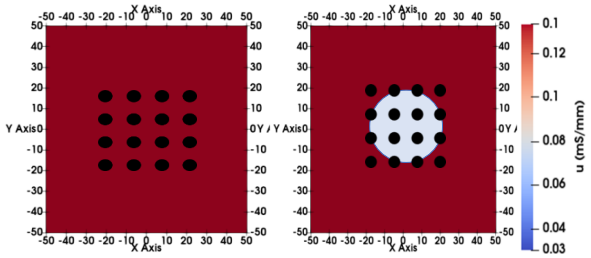

Figure 1. Conductivity of the two-dimensional domain which represents human atrial myocardial tissue (A) Healthy tissue (B) Tissue with region of discrete scar.

Action potential (AP) simulations were carried out using the CardiacEPSolver developed in Nektar++, which uses a high-order spectral/hp element method to solve the monodomain model [15], coupled to the Courtemanche model for the human atrial action potential [16]. The resting potential set for the AP according to the Courtemanche1998 model is -81.00mV. A semi-implicit time-integration method was used for the PDE, forward Euler method was used for numerical integration of ion concentrations and Rush-Larson was used for integrating the gating variables.

The main aim of this study is to understand how changes in the electrode configurations affect the OE morphology. We considered variation in inter-electrode distance and the number of electrodes in a clique. To investigate the effect of inter-electrode distances a clique of 4x4 electrodes was considered at with inter-electrode spacings of 1, 2, 3, 4, 5 and 6mm.

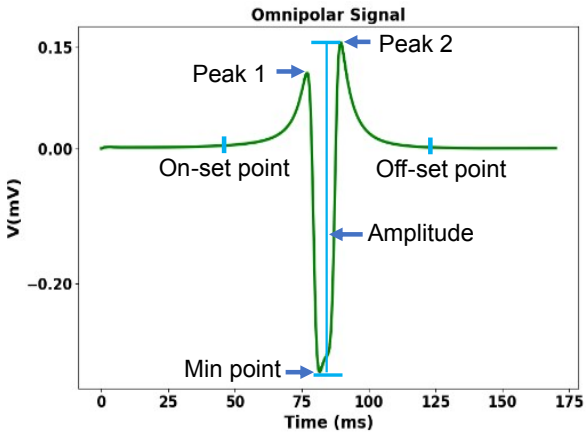

Figure 2. Feature points of the Omnipolar electrogram

UEs were obtained by calculating the extracellular potential at the electrode locations during the simulation. These were used to calculate OEs by estimating the local electric field [13] using the E-field equation,

$$E(t) = E_a(t).a + E_w(t).w; E(t) = E_x(t).x + E_y(t).y \quad (1)$$

For the purpose of calculating OEs, the electrodes and the respective UEs need to be in coplanar. Cliques were selected to derive the local electric fields (E-Field) such as to fully utilise the electrode group. The wavefront propagation within a clique can be calculated from the E-field equation by calculating the wavefront orientation which maximises the cross-correlation of the time and spatial derivatives.

Time-domain features were extracted from the OEs that were calculated under different electrode configurations. Eleven features were calculated through a feature extraction algorithm written in Python 3.8. The time domain features that were considered for this study are shown in Figure 2.

3. Results

We initially consider only the healthy domain. Changes in the voltage-based time-domain features of the OEs with inter-electrode distance is shown in Figure 3. The potential at peak 1 and peak 2 increases as the inter-electrode distance increases monotonically. The voltage at the minimum point (Figure 3 (B) initially decreases, but then increases with electrode distance. The OE amplitude (Figure 3 (D)) consequently follows the reverse. The reason for the reduction of the amplitude is likely due to the separation of contributions of different electrodes, leading to a lower cumulative effect. For an inter-electrode distance of

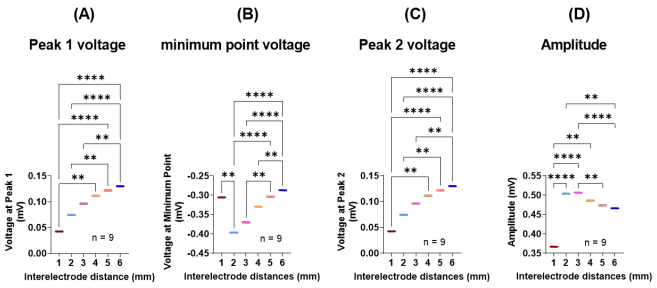

Figure 3. The effect of inter-electrode distance on voltage features of the OEs.

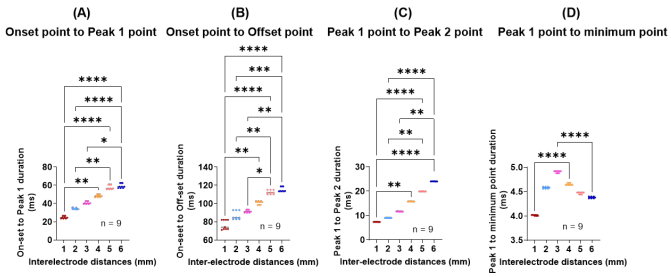

Figure 4. The effect of the inter-electrode distance on the time-intervals between feature points of the OEs.

less than 4mm, the clique of electrodes are all in the active depolarisation stage at the same time leading to a greater cancellation effect between the UEs.

Figure 4 illustrates the effects of the inter-electrode distance on the times between labelled points on the OEs. These intervals gradually increase as the inter-electrode distance increases, except for the interval between Peak 1 and the minimum point. This is due to the depolarisation stage under the clique; with an electrode spacing of 3mm this happens at almost the same time on all the UEs in the clique, while in the clique with 6mm inter-electrode distance, the depolarization stages are delayed.

Figure 5 shows the effect of the number of electrodes in a clique on the voltage features of the OE, for each inter-electrode distance. The voltage of Peak 1 and Peak 2 increases monotonically as the spacing increases, for all clique sizes. The voltage at the minimum point increases as the inter-electrode distance increases across all clique sizes. As observed earlier, the amplitude voltage initially increases slightly but soon decreases as the inter-electrode increased, with only 6mm spacing leading to a monotonically decreasing behaviour.

For time-interval features shown in Figure 6 we observe that the duration between the feature points increases as the inter-electrode distance increases, except for the duration of Peak 1 to Minimum point, for each clique size.

In Figure 7, the morphology of OEs has clear changes as

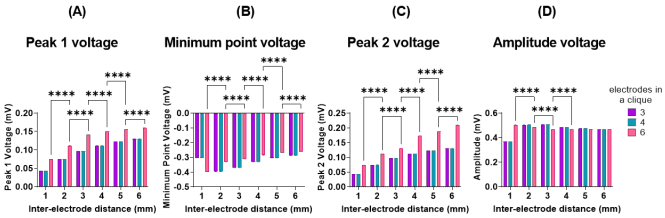

Figure 5. The effect of number of electrodes in a cliques on the voltage recorded from all the features points.

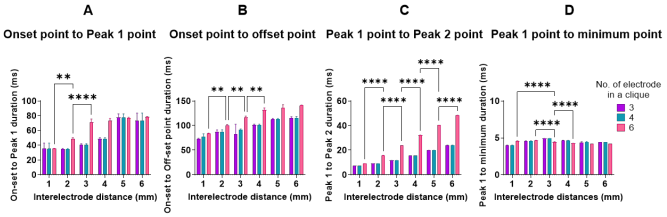

Figure 6. The effect of the number of electrodes in a clique on the intervals of each point labelled on the OEs.

it goes across the scar region; activation is delayed, amplitude is reduced and the OE complex is elongated in time. This is due to the slower conductivity of the scar region which reduces the velocity of the wavefront propagation compared with the healthy region.

4. Discussion

This study examines how the clique electrode configuration and spacing impacts the morphology of OEs. The characteristics of the tissue beneath the electrodes can be determined through the features extracted from the signals. The results suggest the most appropriate inter-electrode distance that can be used to acquire omnipolar electrograms from a myocardial tissue is 2mm or 3mm, while the number are electrodes in each clique is ideally three or four electrodes. Electrode arrangements with less than 2mm inter-electrode spacing, or more than 4mm, were less effective at characterising the underlying domain. Cliques with a higher number of electrodes produce OEs that have a more complex morphology with multiple minima. Inter-electrode spacings of 1mm lead to low-amplitude signals which may be more susceptible to noise.

The OEs of the scar domain have a longer repolarisation time compared to the healthy domain due to the lower effective conductivity of fibrosis slowing wavefront propagation. As well as increasing the overall duration of the electrogram complex, the increased delay between activation at the different clique electrodes leads to increased fractionation which provides a mechanism to quantify scar, but also reduces the effectiveness of the signal for identifying activation times.

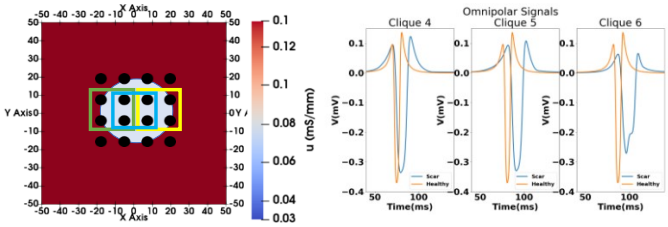

Figure 7. The plot of OEs calculated from healthy domain and scar domain (A) The scar domain with electrodes. Clique 4 (green), clique 5 (blue), clique 6 (yellow). (B) The OEs of healthy (orange) and scar (blue).

5. Conclusion

The distance between the electrodes in the grid is recommended to be less then 4mm and greater than 1mm. The number of electrodes in a clique should be 3 or 4. Further validation in a clinical setting is necessary to ensure translation.

Acknowledgements

MKJL is grateful for support from the British Heart Foundation Centre of Research Excellence.

References

[1] Kornej J, Börschel CS, Benjamin EJ, Schnabel RB. Epidemiology of atrial fibrillation in the 21st century: novel methods and new insights. Circulation research 2020; 127(1):4–20.

[2] Lippi G, Sanchis-Gomar F, Cervellin G. Global epidemiology of atrial fibrillation: an increasing epidemic and public health challenge. International Journal of Stroke 2021; 16(2):217–221.

[3] Krijthe BP, Kunst A, Benjamin EJ, Lip GY, Franco OH, Hofman A, Witteman JC, Stricker BH, Heeringa J. Projections on the number of individuals with atrial fibrillation in the european union, from 2000 to 2060. European heart journal 2013;34(35):2746–2751.

[4] Zoni-Berisso M, Lercari F, Carazza T, Domenicucci S. Epidemiology of atrial fibrillation: European perspective. Clinical epidemiology 2014;6:213.

[5] Bai J, Lo A, Gladding PA, Stiles MK, Fedorov VV, Zhao J. In silico investigation of the mechanisms underlying atrial fibrillation due to impaired pitx2. PLoS computational biology 2020;16(2):e1007678.

[6] Sohns C, Marrouche NF. Atrial fibrillation and cardiac fibrosis. European heart journal 2020;41(10):1123–1131.

[7] Tian J, An X, Niu L. Myocardial fibrosis in congenital and pediatric heart disease. Experimental and therapeutic medicine 2017;13(5):1660–1664.

[8] Chowdhury RA, Tzortzis KN, Dupont E, Selvadurai S, Perbellini F, Cantwell CD, Ng FS, Simon AR, Terracciano CM, Peters NS. Concurrent micro-to macro-cardiac electrophysiology in myocyte cultures and human heart slices. Scientific reports 2018;8(1):1–13.

[9] Verma A, Jiang Cy, Betts TR, Chen J, Deisenhofer I, Mantovan R, Macle L, Morillo CA, Haverkamp W, Weerasooriya R, et al. Approaches to catheter ablation for persistent atrial fibrillation. New England Journal of Medicine 2015;372(19):1812–1822.

[10] Roney CH, Cantwell CD, Siggers JH, Ng FS, Peters NS. A novel method for rotor tracking using bipolar electrogram phase. In Computing in Cardiology 2014. IEEE, 2014; 233–236.

[11] Ragot D, Nayyar S, Massin SZ, Ha AC, Singh SM, Labos C, Suszko A, Dalvi R, Chauhan VS. Unipolar electrogram-based voltage mapping with far-field cancellation to improve detection of abnormal atrial substrate during atrial fibrillation. Journal of Cardiovascular Electrophysiology 2021;32(6):1572–1583.

[12] van Schie MS, Kharbanda RK, Houck CA, Lanters EA, Taverne YJ, Bogers AJ, de Groot NM. Identification of low-voltage areas: A unipolar, bipolar, and omnipolar perspective. Circulation Arrhythmia and Electrophysiology 2021; 14(7):e009912.

[13] Deno DC, Bhaskaran A, Morgan DJ, Goksu F, Batman K, Olson GK, Magtibay K, Nayyar S, Porta-Sánchez A, Laflamme MA, et al. High-resolution, live, directional mapping. Heart Rhythm 2020;17(9):1621–1628.

[14] Takigawa M, Kitamura T, Basu S, Bartal M, Martin CA, Martin R, Cheniti G, Vlachos K, Pillois X, Frontera A, et al. Effect of electrode size and spacing on electrograms: Optimized electrode configuration for near-field electrogram characterization. Heart rhythm 2022;19(1):102–112.

[15] Cantwell CD, Yakovlev S, Kirby RM, Peters NS, Sherwin SJ. High-order spectral/hp element discretisation for reaction–diffusion problems on surfaces: Application to cardiac electrophysiology. Journal of computational physics 2014;257:813–829.

[16] Courtemanche M, Ramirez RJ, Nattel S. Ionic mechanisms underlying human atrial action potential properties: insights from a mathematical model. American Journal of Physiology Heart and Circulatory Physiology 1998; 275(1):H301–H321.

Address for correspondence:

Name: Chris D. Cantwell
Full postal address: Room 219, Department of Aeronautics, City and Guilds Building, South Kensington Campus
E-mail address (optional):c.cantwell@imperial.ac.uk